



Cite this: DOI: 10.1039/d1dt00924a

# Multinuclear transition metal-containing polyoxometalates constructed from Nb/W mixed-addendum precursors: synthesis, structures and catalytic performance†

Wanru Xiao,<sup>a</sup> Shujun Li,<sup>a</sup>  \*<sup>a</sup> Yue Zhao,<sup>a</sup> Yubin Ma,<sup>a</sup> Na Li,<sup>a</sup> Jie Zhang <sup>a</sup> and Xuenian Chen  \*<sup>a,b</sup>

Four new transition metal-containing Nb/W mixed-addendum POM trimers with the formula  $H_{19}[M_4(H_2O)_x(P_2W_{15}Nb_3O_{62})_3] \cdot m(HCOOH) \cdot nH_2O$  ( $M = Cu$ ,  $x = 15$ ,  $m = 0$ , and  $n = 21$ , **Cu-POM**;  $M = Co$ ,  $x = 7$ ,  $m = 0$ , and  $n = 15$ , **Co-POM**;  $M = Mn$ ,  $x = 7$ ,  $m = 6$ , and  $n = 18$ , **Mn-POM**; and  $M = Zn$ ,  $x = 7$ ,  $m = 0$ , and  $n = 23$ , **Zn-POM**) have been synthesized by a solvothermal method in a water–ethanol mixed solvent. All the four compounds were characterized by single-crystal X-ray diffraction, powder X-ray diffraction (XRD), IR spectroscopy, thermogravimetric analysis (TGA), and X-ray photoelectron spectroscopy (XPS). These compounds can serve as efficient heterogeneous catalysts for the cyanosilylation of different carbonyl compounds under ambient temperature and solvent-free conditions, and **Cu-POM** shows much better catalytic performance than the other three compounds. The cycle experiment showed that **Cu-POM** can be reused for at least five cycles without significant loss of catalytic activity. The IR spectroscopy and XRD analysis revealed that **Cu-POM** can retain its integrity after catalysis.

Received 21st March 2021

Accepted 28th April 2021

DOI: 10.1039/d1dt00924a

rsc.li/dalton

## Introduction

Transition-metal-substituted POMs (TMSPs) as a large subclass of polyoxometalates (POMs) are attracting considerable attention in recent years.<sup>1–3</sup> The replacement of 3d transition metal (TM) ions Mn, Co, Ni, Cu, *etc.* in POMs results in abundant structure diversity, for instance mono- and multi-substituted and high-nuclear metal-substituted derivatives, and fascinating properties applicable to magnetism,<sup>4–7</sup> catalysis,<sup>8–11</sup> electrochemistry,<sup>12–14</sup> medicine and materials science.<sup>15–17</sup>

An effective synthesis approach to TMSPs is utilizing the reactions of lacunary POM precursors (such as lacunary Keggin  $[XW_9O_{34}]^{9/10-}$  ( $X = P^V/Si^{IV}/Ge^{IV}$ ) or Dawson  $[P_2W_{15}O_{56}]^{12-}$ ) and TM ions.<sup>18</sup> A typical example is the synthesis of the first sand-

wich-type polyoxometalate  $[Co_4(H_2O)_2(B-\alpha-PW_9O_{34})_2]^{10-}$  in 1973.<sup>19</sup> In addition, the self-assembly of metal salts or metal oxides (*e.g.*  $Na_2WO_4$  and  $WO_3$ ) with TMs was also used to construct the TMSP structure. Mialane and co-workers obtained two Fe-substituted compounds  $[Fe_4(H_2O)_2(FeW_9O_{34})_2]^{10-}$  and  $[(Fe_4W_9O_{34}(H_2O))_2(FeW_6O_{26})]^{19-}$  by the reaction of  $Na_2WO_4$  and  $FeCl_3$ .<sup>20</sup> From the experimental point of view, conventional aqueous solution synthesis and hydrothermal synthesis are the most common methods for these TMSPs due to their relatively simple synthesis process. However, a solvothermal method was rarely used in the synthesis of TMSPs.

Mixed-addendum POMs as a branch of POMs have received increasing attention because they can serve as excellent precursors to react with nucleophilic reagents. The substitution of  $Nb^V/Ta^V$  for  $W^{VI}$  will raise the charge of the whole polyoxoanion and endow the POMs with high reactivity due to the increased nucleophilicity and basicity of the O atoms connected to Nb or Ta.<sup>21</sup> Utilizing these features, a series of compounds based on Nb (Ta)/W mixed-addendum POMs have been synthesized, for example, Nb/W mixed-addendum POM-supported organometallic complexes,<sup>22–24</sup> lanthanide-functional POMs,<sup>21,25</sup> boronic acid covalent functionalized POMs,<sup>26</sup> and boronic acid modified Ln–POMs.<sup>27</sup>

In this work, we obtained four POM trimers, which were synthesized by the reaction of the Nb/W mixed-addendum POM  $[P_2W_{15}Nb_3O_{62}]^{9-}$  and TM ions ( $Cu^{2+}$ ,  $Co^{2+}$ ,  $Mn^{2+}$ ,  $Zn^{2+}$ )

<sup>a</sup>School of Chemistry and Chemical Engineering, Henan Key Laboratory of Boron Chemistry and Advanced Energy Materials, Key Laboratory of Green Chemical Media and Reactions, Ministry of Education, Collaborative Innovation Centre of Henan Province for Green Manufacturing of Fine Chemicals, Henan Normal University, Xinxiang, 453007, China. E-mail: lijsj@htu.edu.cn

<sup>b</sup>College of Chemistry and Molecular Engineering Zhengzhou University, Zhengzhou, 450001, China. E-mail: xnchen@htu.edu.cn

† Electronic supplementary information (ESI) available: Experimental procedures, crystallographic structures, FTIR spectroscopy, thermal analyses, PXRD patterns, and catalytic data for the title compounds. CCDC 2044367–2044370. For ESI and crystallographic data in CIF or other electronic format see DOI: 10.1039/d1dt00924a

under solvothermal conditions. The resulting compounds display a trimeric structure linked by four metal ions forming the structure of POMs with Lewis acid metal centers. **Co-POM**, **Mn-POM**, and **Zn-POM** show isomorphous structures, in which the metal ions are tetrahedrally coordinated, while the Cu ions in **Cu-POM** exhibit octahedral coordination. **Cu-POM** was proved to be an efficient heterogeneous catalyst for the cyanosilylation reaction under ambient temperature and solvent-free conditions, and displayed excellent cyclability in the catalytic process.

## Results and discussion

### Synthetic considerations

All the four compounds were synthesized by a solvothermal method using a Nb/W mixed-addendum Dawson-type precursor ( $\text{K}_8\text{H}[\text{P}_2\text{W}_{15}(\text{NbO}_2)_3\text{O}_{59}]\cdot 12\text{H}_2\text{O}$ ) and the corresponding transition metal salts ( $\text{Cu}(\text{NO}_3)_2\cdot 3\text{H}_2\text{O}$ ,  $\text{CoCl}_2\cdot 6\text{H}_2\text{O}$ , and  $\text{MnCl}_2$ ,  $\text{Zn}(\text{NO}_3)_2\cdot 6\text{H}_2\text{O}$ ) in a  $\text{H}_2\text{O}/\text{EtOH}$  mixed solvent. Many factors including solvents, the reaction temperature and time and pH of the mixed solution have been reported to have important influence on the synthesis of POM compounds.<sup>28</sup> In our case, the proportion of the solvents ( $V_{\text{H}_2\text{O}}:V_{\text{EtOH}} = 2:1$ ) is crucial for the production of the title compounds. Higher proportion of ethanol (*e.g.*  $V_{\text{H}_2\text{O}}:V_{\text{EtOH}} = 1:1$  or  $1:2$ ) can only result in the formation of an unidentifiable precipitate.

For the synthesis of **Cu-POM**, **Co-POM** and **Mn-POM**, formic acid is essential. No expected product can be obtained when acetic acid or hydrochloric acid is used. However, acetic acid is important for the synthesis of **Zn-POM**, whose yield is poor when acetic acid is replaced by formic acid. The four compounds can only be obtained with a given amount of the acid (2.5 mL for **Cu-POM**, 7 mL for **Co-POM**, 4.5 mL for **Mn-POM** and 5 mL for **Zn-POM**). Although formic acid and acetic acid do not appear in the final structure of the title compounds (except for **Mn-POM**), they play important roles in the formation of the four compounds. Firstly, the pH of the solution is a key factor for the synthesis of POMs. The specific acidic environment produced by a certain amount of an acid is necessary for the syntheses of the reported TM-POMs with different TM ions. Secondly, formic acid and acetic acid may combine with TM ions in the reaction solutions. So, the amount/concentration and type of acid are related to the coordination equilibrium, which may affect the reaction of TM ions with POMs and affect the final formation of the TM-POMs.

### Structural description

Single-crystal X-ray diffraction analysis (Table S1<sup>†</sup>) indicates that all the four compounds crystallize in trigonal symmetry,  $P\bar{3}$  space group. They exhibit similar structures with the only difference in the coordination of the TM ions. As shown in Fig. 1a and Fig. S1–S3,<sup>†</sup> the asymmetrical unit of **Cu-POM** contains three  $\{\text{P}_2\text{W}_{15}\text{Nb}_3\text{O}_{62}\}$ , three  $[\text{Cu}(\text{H}_2\text{O})_4]^{2+}$  and one  $[\text{Cu}(\text{H}_2\text{O})_3]^{2+}$  to form a trimer, in which Cu1 connects three polyox-

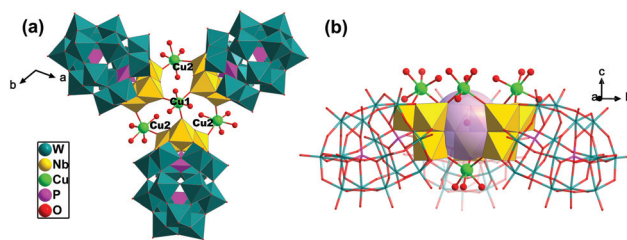


Fig. 1 Combined polyhedral/ball-and-stick representation of (a) the asymmetrical unit of **Cu-POM**, view along the *c* axis; (b) the flat cluster view along the *a* axis, highlighting the bowl-shaped centre and the hollow (pink ball) in the bowl.

anions through three Cu1–O2–Nb1 bridges with the Cu1–O2 bond length of 1.993 Å. Cu1 is located at the  $C_3$  axis of the whole structure. The remaining three Cu2 connect two of the polyoxoanions in the structure through Cu2–O7–Nb2 and Cu2–O8–Nb3, with the bond lengths of Cu2–O7 and Cu2–O8 being 2.190 Å and 1.963 Å, respectively (Fig. S1<sup>†</sup>). Both Cu1 and Cu2 exhibit a six-coordinate octahedral configuration (Fig. S1b<sup>†</sup>). Alternatively, this novel trimer can be viewed as a flat cluster, with all the Cu and coordination water molecules of Cu exposed to the two sides of the flat cluster (Fig. 1b).

**Co-POM**, **Mn-POM** and **Zn-POM** are isostructural, but their asymmetrical structure characteristics are different from those of **Cu-POM**: all the  $\text{Co}^{2+}$ ,  $\text{Mn}^{2+}$  and  $\text{Zn}^{2+}$  ions in these compounds adopt tetrahedral coordination. Taking **Zn-POM** as an example (Fig. 2a and Fig. S4<sup>†</sup>), each polyanion contains three  $\{\text{P}_2\text{W}_{15}\text{Nb}_3\text{O}_{62}\}$ , three  $[\text{Zn}(\text{H}_2\text{O})_2]^{2+}$  and one  $[\text{Zn}(\text{H}_2\text{O})]^{2+}$ . Both Zn1 and Zn2 exhibit a four-coordinate tetrahedral configuration (Fig. S4b<sup>†</sup>).

In the centre of all the four compounds, three  $\{\text{Nb}_3\}$  clusters and four TM ions are linked alternately forming a bowl (Fig. 1b and 2b). There is a hollow in the bowl with a diameter of about 9 Å, in the centre of which a water molecule is locked (Fig. S2<sup>†</sup>). As shown in Table S2,<sup>†</sup> bond valence sum (BVS) analyses reveal that the bond valences for all the terminal O atoms of the TM sites are in the range of 0.283 to 0.472, indicating that all of them exist in the form of coordination water,<sup>10</sup> and the BVS value of all the other O atoms in the POM skeleton is  $-2$ . BVS analyses for the other elements in these compounds

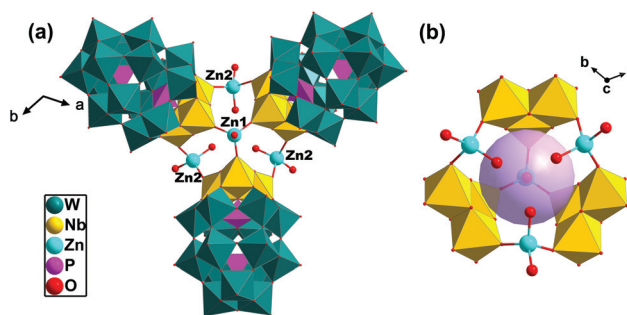


Fig. 2 Combined polyhedral/ball-and-stick representation of (a) the asymmetrical unit of **Zn-POM**; (b) the hollow (pink ball) in the bowl.

indicated the following oxidation states: W(vi), Nb(v), P(v), Cu(II), Co(II), Mn(II), and Zn(II) (Table S3†).

### X-ray photoelectron spectroscopy (XPS)

The oxidation states of the TM ions ( $\text{Cu}^{2+}$ ,  $\text{Co}^{2+}$ ,  $\text{Mn}^{2+}$ , and  $\text{Zn}^{2+}$ ) in the title compounds were further confirmed by XPS spectroscopy. The peaks at 952.8 eV and 933.1 eV for **Cu-POM** can be assigned to  $\text{Cu}^{2+}$  2p<sub>1/2</sub> and  $\text{Cu}^{2+}$  2p<sub>3/2</sub>, respectively (Fig. 3a).<sup>29</sup> The peaks at 797.5 eV and 781.2 eV for **Co-POM** represent  $\text{Co}^{2+}$  2p<sub>1/2</sub> and  $\text{Co}^{2+}$  2p<sub>3/2</sub>, respectively (Fig. 3b).<sup>30</sup> As shown in Fig. 3c, two Mn 2p photoelectron peaks occurring at 654.6 eV and 641.9 eV correspond to the characteristic peak positions of  $\text{Mn}^{2+}$ . The representative peaks of the Zn 2p spectrum at 1045.2 eV and 1022.1 eV correspond to  $\text{Zn}^{2+}$  2p<sub>1/2</sub> and  $\text{Zn}^{2+}$  2p<sub>3/2</sub>, respectively (Fig. 3d).<sup>31</sup> The oxidation states of these metal ions were fully consistent with the BVS analysis results (Table S3†). The binding energies of the transition elements in **Co-POM**, **Mn-POM** and **Zn-POM** are slightly higher than the binding energies of those in their corresponding oxides, which may be related to the coordination environment and the surrounding charge density of the metal ions in these compounds. Generally, metal ions will have less stability in tetrahedral positions which will result in higher values of binding energy.<sup>32,33</sup> Besides, the coordination of these TM ions with high-negative POMs may decrease the electron density around them, which will also result in their higher binding energies.<sup>34</sup>

### Catalytic activities

The cyanosilylation of carbonyl compounds is an important reaction in organic synthesis for producing cyanohydrin derivatives, which have been widely utilized as important synthetic intermediates for organic compounds. Lewis acid catalysts can act as electrophilic catalysts to activate carbonyl compounds. Several nucleophilic catalysts, such as amines, phosphines, and alkaline earth metal oxides, can activate TMSCN

and promote cyanosilylation.<sup>35,36</sup> The open coordination environment of the TM and the labile coordination water in the four title compounds may afford Lewis acid active sites. Besides,  $\{\text{P}_2\text{W}_{15}\text{Nb}_3\text{O}_{62}\}$  possesses bare nucleophilic surfaces as a result of external oxygen atoms, which can act as a Lewis base. Based on the synergy between them, we tested the activity of the four compounds as heterogeneous catalysts in the cyanosilylation reaction under solvent-free conditions at room temperature.

**Optimization of the catalyst.** The cyanosilylation of benzaldehyde was chosen as a model reaction to evaluate different catalysts and optimize the conditions. First, we investigated the catalytic activity of the four compounds in the reaction with 1 mol% of catalysts. The yield of 2-phenyl-2-((trimethylsilyl)oxy)acetonitrile reached 91.7% after 2.5 h when **Cu-POM** was used as the catalyst, while the yields with the other three compounds were less than 80% for the same reaction time (Table 1, entries 1–4). The conversion curves of the four compounds also indicated that **Cu-POM** possesses

**Table 1** Optimization of the parameters of the cyanosilylation reaction of benzaldehyde and TMSCN<sup>a</sup>

Entry	Catalyst (mol%)	Time (h)	Yield <sup>b</sup> (%)
1	<b>Cu-POM</b>	2.5	91.7
2	<b>Co-POM</b>	2.5	78.9
3	<b>Mn-POM</b>	2.5	72.5
4	<b>Zn-POM</b>	2.5	61.3
5	<b>Cu-POM</b> (unactivated)	2.5	51.2
6	<b>Cu-POM</b> (0.3)	2.5	50.5
7	<b>Cu-POM</b> (0.5)	2.5	98.0
8	$\{\text{P}_2\text{W}_{15}\text{Nb}_3\}$	2.5	18.0
9	$\text{Cu}(\text{NO}_3)_2 \cdot 3\text{H}_2\text{O}$	2.5	1.02
10	$\{\text{P}_2\text{W}_{15}\text{Nb}_3\}/\text{Cu}$	2.5	39.2

<sup>a</sup> Reaction conditions: 0.5 mmol of aldehydes, 1.5 mmol of TMSCN, 1.0 mol% of catalyst, without solvent, room temperature (25 °C), under  $\text{N}_2$ . <sup>b</sup> Yields were determined by <sup>1</sup>H NMR.

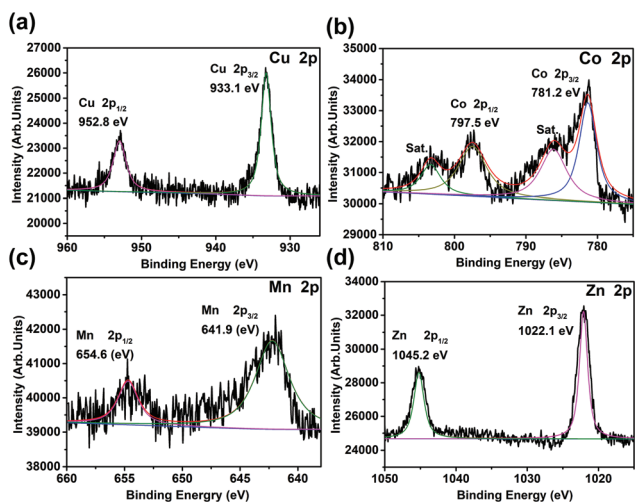


**Fig. 3** XPS spectra of Cu 2p (a), Co 2p (b), Mn 2p (c) and Zn 2p (d) in the title compounds.

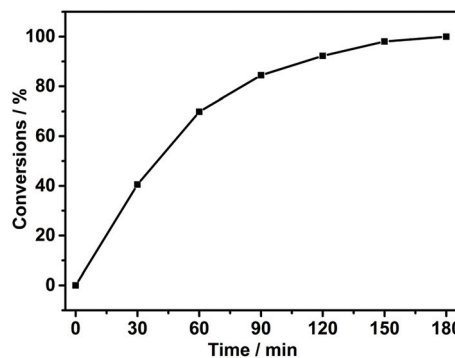
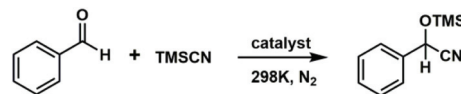


**Fig. 4** Conversion curve of the cyanosilylation reaction of benzaldehyde with **Cu-POM** (0.5 mol%) as the catalyst.

superior catalytic activity to the other three compounds in cyanosilylation (Fig. S8†). Without activation, **Cu-POM** can catalyze the reaction with a low yield (51.2%, Table 1, entry 5), which suggests that the activation of the catalyst is conducive to the catalytic reaction probably owing to the exposure of unsaturated coordination active sites after being heated.

**Table 2** Cyanosilylation of various carbonyl compounds with TMSCN<sup>a</sup>

Entry	Substrate	Product	Yield <sup>b</sup> (%)
1			98.0
2			99.9
3			99.8
4			99.7
5			93.4 <sup>c</sup>
6			86.9
7			72.4
8			87.8 <sup>c</sup>
9			79.3
10			54.0
11			Trace
12			Trace

<sup>a</sup> Reaction conditions: 0.5 mmol of aldehydes, 1.5 mmol of TMSCN, 0.5 mol% of catalyst, without solvent, room temperature (25 °C), under N<sub>2</sub> for 2.5 h. <sup>b</sup> Yields were determined by <sup>1</sup>H NMR. <sup>c</sup> Isolated yields. Entries 5 and 8 were selected for purification to obtain pure products: after the reaction, the mixture was purified by column chromatography over silica gel (100–200 mesh) using an ethyl acetate/petroleum ether (1 : 10) mixture as an eluent to obtain pure products.<sup>41</sup>

Generally, the reaction activity is positively correlated with the catalyst dosage; a higher dosage is beneficial for the conversions.<sup>37</sup> However, in this work, with the increasing amount of the catalyst (from 0.5 mol% to 1 mol%), the yield decreased from 98.0% to 91.7% (Table 1, entries 1 and 7). Increasing the catalyst loading does not provide any substantial benefits to the reaction efficiency obviously. A similar phenomenon has been reported by the Wei group.<sup>38</sup> The catalytic activities of the precursors {P<sub>2</sub>W<sub>15</sub>Nb<sub>3</sub>} and Cu(NO<sub>3</sub>)<sub>2</sub>·3H<sub>2</sub>O are far lower than that of **Cu-POM**. Obviously, the catalytic activity of the {P<sub>2</sub>W<sub>15</sub>Nb<sub>3</sub>}/Cu mixture is better than that of any single constituent, indicating that there would be a synergy between them (Table 1, entries 8–10).<sup>37</sup> Conversion of cyanohydrin trimethylsilyl ether *vs.* reaction time catalyzed by **Cu-POM** (0.5 mol%) was investigated due to the good catalytic performance. As shown in Fig. 4, the conversion of benzaldehyde increased significantly within 2 h (92.2%) and varied from 92.2% to 99.9% in the following 1 h, demonstrating that the reaction was almost completed after two hours.

**Scope of the substrate.** The cyanosilylation of different aldehydes/ketones with TMSCN catalyzed by **Cu-POM** was further studied. As shown in Table 2, when the substrate is 4-fluorobenzaldehyde, 4-nitrobenzaldehyde or 4-cyanobenzaldehyde, the yields are over 99% (Table 2, entries 2–4). For substrates like 4-methylbenzaldehyde and 4-methoxybenzaldehyde, the resulting yields are relatively low (Table 2, entries 8 and 9). This indicates that the nature of the substituent on the aromatic ring may dramatically affect the reaction yields. The activity of substrates with electron-withdrawing substituents is higher than the activity of those with electron-donating substituents, resulting from an increase of the substrate electrophilicity in the former case.<sup>39,40</sup> In addition, steric hindrance has an influence on the yields, *para*-substituent > *meta*-substituent > *ortho*-substituent, obviously (Table 2, entries 5–7). A low yield (54.0%) is observed when 1-naphthaldehyde is used as the substrate which has larger steric hindrance (Table 2, entry 10). The activity of ketones is much lower with final yields of less than 1% (Table 2, entries 11 and 12).

**Recyclability and stability.** The recyclability of **Cu-POM** as a catalyst was investigated. After the catalytic reaction, the catalyst was separated and reused for the next round. It could be used for five cycles with no significant decrease in the conver-

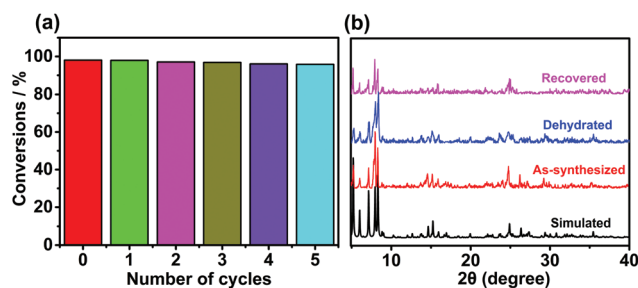


**Fig. 5** (a) Recyclability of **Cu-POM** as the catalyst for the cyanosilylation of benzaldehyde. (b) Powder XRD patterns of the simulated (black), as-synthesized (red), dehydrated (blue) and recovered (pink) **Cu-POM**.

sions (Fig. 5a). Meanwhile, the PXRD patterns (Fig. 5b) and the IR spectra (Fig. S9†) of the recovered **Cu-POM** remained unchanged, which proved that the polyoxoanion of **Cu-POM** is stable and the crystal lattice is mainly retained after catalysis.

## Conclusions

In conclusion, we have successfully synthesized four POM trimers from Nb/W mixed-addendum POMs and TM ions ( $\text{Cu}^{2+}$ ,  $\text{Co}^{2+}$ ,  $\text{Mn}^{2+}$ , and  $\text{Zn}^{2+}$ ) under solvothermal conditions. They were composed of three  $\{\text{P}_2\text{W}_{15}\text{Nb}_3\}$  units and four  $[\text{M}(\text{H}_2\text{O})_x]^{2+}$  groups resulting in trimeric aggregates. The catalytic investigation revealed that **Cu-POM** showed higher efficiency compared to **Co-POM**, **Mn-POM** and **Zn-POM**. **Cu-POM** can be reused for five cycles without significant reduction in its catalytic activity. These results exemplify the potential of using mixed-addendum POMs and transition metals to form the structures of POMs with Lewis acid metal centers which further enhance their catalytic activity.

## Author contributions

W. Xiao and Y. Zhao co-worked on the synthesis and characterization of the title compounds. W. Xiao and Y. Ma performed the catalytic experiments. S. Li and J. Zhang collected the structural data and provided detailed refinements on the crystal structures. S. Li and X. Chen conceived the project and designed the experiments. All authors co-wrote the manuscript.

## Conflicts of interest

There are no conflicts to declare.

## Acknowledgements

This work was supported by the National Natural Science Foundation of China (U1804253), the Natural Science Foundation of Henan Province (202300410246) and the breeding programs of Henan Normal University (2019PL06).

## Notes and references

- S.-T. Zheng and G.-Y. Yang, *Chem. Soc. Rev.*, 2012, **41**, 7623–7646.
- O. Oms, A. Dolbecq and P. Mialane, *Chem. Soc. Rev.*, 2012, **41**, 7497–7536.
- M. Ibrahim, Y. Xiang, B. S. Bassil, Y. Lan, A. K. Powell, P. de Oliveira, B. Keita and U. Kortz, *Inorg. Chem.*, 2013, **52**, 8399–8408.
- U. Kortz, A. Müller, J. van Slageren, J. Schnack, N. S. Dalal and M. Dressel, *Coord. Chem. Rev.*, 2009, **253**, 2315–2327.
- J. M. Clemente-Juan, E. Coronado and A. Gaita-Ariño, *Chem. Soc. Rev.*, 2012, **41**, 7464–7478.
- J. Jiang, Y. Chen, L. Liu, L. Chen and J. Zhao, *Inorg. Chem.*, 2019, **58**, 15853–15863.
- S.-Y. Wu, Y.-J. Wang, J.-X. Jing, X.-X. Li, Y.-Q. Sun and S.-T. Zheng, *Inorg. Chem. Front.*, 2020, **7**, 498–504.
- Y. Chen, Z.-W. Guo, Y.-P. Chen, Z.-Y. Zhuang, G.-Q. Wang, X.-X. Li, S.-T. Zheng and G.-Y. Yang, *Inorg. Chem. Front.*, 2021, **8**, 1303–1311.
- A. Sartorel, M. Bonchio, S. Campagna and F. Scandola, *Chem. Soc. Rev.*, 2013, **42**, 2262–2280.
- J. Jia, Y. Niu, P. Zhang, D. Zhang, P. Ma, C. Zhang, J. Niu and J. Wang, *Inorg. Chem.*, 2017, **56**, 10131–10134.
- Y.-S. Ding, H.-Y. Wang and Y. Ding, *Dalton Trans.*, 2020, **49**, 3457–3462.
- L.-H. Bi, G. Al-Kadamany, E. V. Chubarova, M. H. Dickman, L. Chen, D. S. Gopala, R. M. Richards, B. Keita, L. Nadjo, H. Jaensch, G. Mathys and U. Kortz, *Inorg. Chem.*, 2009, **48**, 10068–10077.
- S.-X. Guo, C.-Y. Lee, J. Zhang, A. M. Bond, Y. V. Geletii and C. L. Hill, *Inorg. Chem.*, 2014, **53**, 7561–7570.
- X. Xin, N. Hu, Y. Ma, Y. Wang, L. Hou, H. Zhang and Z. Han, *Dalton Trans.*, 2020, **49**, 4570–4577.
- A. Proust, R. Thouvenot and P. Gouzerh, *Chem. Commun.*, 2008, 1837–1852.
- D.-L. Long, E. Burkholder and L. Cronin, *Chem. Soc. Rev.*, 2007, **36**, 105–121.
- S. Shigeta, S. Mori, T. Yamase, N. Yamamoto and N. Yamamoto, *Biomed. Pharmacother.*, 2006, **60**, 211–219.
- X.-X. Li, W.-H. Fang, J.-W. Zhao and G.-Y. Yang, *Chem. – Eur. J.*, 2014, **20**, 17324–17332.
- T. J. R. Weakley, H. T. Evans, J. S. Showell, G. F. Tourné and C. M. Tourné, *J. Chem. Soc., Chem. Commun.*, 1973, 139–140.
- J. D. Compain, P. Mialane, A. Dolbecq, I. M. Mbomekalle, J. Marrot, F. Secheresse, E. Riviere, G. Rogez and W. Wernsdorfer, *Angew. Chem., Int. Ed.*, 2009, **48**, 3077–3081.
- S.-J. Li, S.-X. Liu, N.-N. Ma, Y.-Q. Qiu, J. Miao, C.-C. Li, Q. Tang and L. Xu, *CrystEngComm*, 2012, **14**, 1397–1404.
- M. Pohl, D. K. Lyon, N. Mizuno, K. Nomiya and R. G. Finke, *Inorg. Chem.*, 1995, **34**, 1413–1429.
- N. Mizuno, D. K. Lyon and R. G. Finke, *J. Catal.*, 1991, **128**, 84–91.
- H. Weiner, A. Trovarelli and R. G. Finke, *J. Mol. Catal. A: Chem.*, 2003, **191**, 253–279.
- S. Li, Y. Zhou, Q. Peng, R. Wang, X. Feng, S. Liu, X. Ma, N. Ma, J. Zhang, Y. Chang, Z. Zheng and X. Chen, *Inorg. Chem.*, 2018, **57**, 6624–6631.
- S. Li, Y. Zhou, N. Ma, J. Zhang, Z. Zheng, C. Streb and X. Chen, *Angew. Chem., Int. Ed.*, 2020, **59**, 8537–8540.
- S. Li, Y. Zhao, H. Qi, Y. Zhou, S. Liu, X. Ma, J. Zhang and X. Chen, *Chem. Commun.*, 2019, **55**, 2525–2528.
- J.-P. Cao, Y.-S. Xue, Z.-B. Hu, X.-M. Luo, C.-H. Cui, Y. Song and Y. Xu, *Inorg. Chem.*, 2019, **58**, 2645–2651.
- D. P. Shoemaker, J. Li and R. Seshadri, *J. Am. Chem. Soc.*, 2009, **131**, 11450–11457.

- 30 J. Wang, P. Ma and J. Niu, *Sci. China, Ser. B: Chem.*, 2007, **50**, 784–789.
- 31 T. Liu, J. Liu, Q. Liu, D. Song, H. Zhang, H. Zhang and J. Wang, *Nanoscale*, 2015, **7**, 19714–19721.
- 32 C. Elmi, S. Guggenheim and R. Gieré, *Clays Clay Miner.*, 2016, **64**, 537–551.
- 33 P. N. Lisboa-Filho, C. Vila, M. S. Góes, C. Morilla-Santos, L. Gama, E. Longo, W. H. Schreiner and C. O. Paiva-Santos, *Mater. Chem. Phys.*, 2004, **85**, 377–382.
- 34 S.-R. Ye, Y.-K. Shan and L.-Y. Dai, *J. Coord. Chem.*, 2006, **57**, 145–155.
- 35 Y. Kikukawa, K. Suzuki, M. Sugawa, T. Hirano, K. Kamata, K. Yamaguchi and N. Mizuno, *Angew. Chem., Int. Ed.*, 2012, **51**, 3686–3690.
- 36 H. An, J. Zhang, S. Chang, Y. Hou and Q. Zhu, *Inorg. Chem.*, 2020, **59**, 10578–10590.
- 37 D. Li, Q. Xu, Y. Li, Y. Qiu, P. Ma, J. Niu and J. Wang, *Inorg. Chem.*, 2019, **58**, 4945–4953.
- 38 D. Dan, F. Chen, W. Zhao, H. Yu, S. Han and Y. Wei, *Dalton Trans.*, 2021, **50**, 90–94.
- 39 A. G. Mahmoud, K. T. Mahmudov, M. F. C. Guedes da Silva and A. J. L. Pombeiro, *RSC Adv.*, 2016, **6**, 54263–54269.
- 40 J.-Z. Gu, S.-M. Wan, M. V. Kirillova and A. M. Kirillov, *Dalton Trans.*, 2020, **49**, 7197–7209.
- 41 W. Wang, M. Luo, W. Yao, M. Ma, S. A. Pullarkat, L. Xu and P.-H. Leung, *ACS Sustainable Chem. Eng.*, 2019, **7**, 1718–1722.